JACS
JOURNAL OF THE AMERICAN CHEMICAL SOCIETY
Communication
pubs.acs.org/JACS

Conversion of Fe−NH_2 to Fe−N_2 with release of NH_3

John S. Anderson, Marc-Etienne Moret, and Jonas C. Peters*

Division of Chemistry and Chemical Engineering, California Institute of Technology, Pasadena, California 91125, United States

Supporting Information

ABSTRACT: Tris(phosphine)borane ligated Fe(I) centers featuring N_2H_4, NH_3, NH_2, and OH ligands are described. Conversion of Fe−NH_2 to Fe−NH_3^+ by the addition of acid, and subsequent reductive release of NH_3 to generate Fe−N_2, is demonstrated. This sequence models the final steps of proposed Fe−mediated nitrogen fixation pathways. The five-coordinate trigonal bipyramidal complexes described are unusual in that they adopt S = 3/2 ground states and are prepared from a four-coordinate, S = 3/2 trigonal pyramidal precursor.

Due to the structural and mechanistic complexity of biological nitrogen fixation[1] a variety of mechanisms have been proposed that invoke either Mo or Fe as the likely active site for N_2 binding and reduction. Fe−NH_2 is an intermediate common to both limiting mechanisms (i.e., distal vs alternating) being considered for Fe−mediated N_2 fixation scenarios at the FeMo-cofactor.[2,3] Such a species could form via reductive protonation of the nitride intermediate of a distal scheme (i.e., Fe(N) → Fe(NH) → Fe(NH_2) → Fe(NH_3)), or by reductive protonation of a hydrazine intermediate of an alternating scheme (i.e., Fe(NH_2−NH_2) → Fe(NH_2) + NH_3). In this context, detection of an EPR active Fe−NH_2 or possibly Fe−NH_3 common intermediate has been proposed under reducing conditions at the FeMo-cofactor from substrates including N_2, N_2H_4, and MeN═NH.[3a]

One key to realizing a catalytic cycle in either limiting scenario concerns the regeneration of Fe−N_2 from Fe−NH_2 with concurrent release of NH_3.[4] While there have been recent synthetic reports demonstrating NH_3 generation from Fe(N) nitride model complexes, these studies have not provided information about the plausible downstream Fe(NH_x) (X = 1, 2, 3) intermediates en route to NH_3 release, nor have these systems illustrated the feasibility of regeneration of Fe−N_2.[5] Herein we describe a terminal, S = 3/2 Fe−NH_2 complex for which the stepwise conversion to Fe−NH_3, and then to Fe−N_2 along with concomitant release of NH_3, is demonstrated (eqs 1 and 2).

$$\mathrm{Fe-NH_2} + \mathrm{H^+} \rightarrow \mathrm{Fe-NH_3^+} \quad (1)$$

$$\mathrm{Fe-NH_3^+} + \mathrm{e^-} + \mathrm{N_2} \rightarrow \mathrm{Fe-N_2} + \mathrm{NH_3} \quad (2)$$

The addition of methyllithium to (TPB)FeBr[6] affords the corresponding methyl complex (TPB)FeMe (**1**) in high yield (Scheme 1). Protonation of **1** by $HBAr^F_4{\cdot}2Et_2O$ ($BAr^F_4{}^-$ = $B(3,5\text{-}C_6H_3(CF_3)_2)_4^-$) in a cold ethereal solution releases methane to yield [(TPB)Fe][BAr^F_4] (**2**) which serves as a useful synthon with a vacant coordination site.

Scheme 1

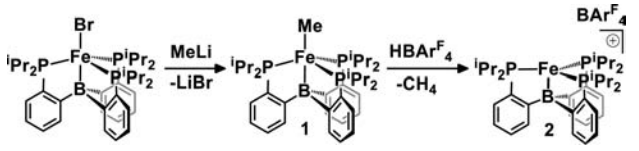

XRD data were obtained for **1** and **2** (Figure 1). The geometry of **1** is pseudotrigonal bipyramidal about Fe with an Fe−C bond length of 2.083(10) Å and an Fe−B bond length of 2.522 (2) Å. In the solid state **2** possesses a four-coordinate distorted trigonal pyramidal geometry with no close contacts in the apical site trans to boron, making this complex coordinatively unsaturated. Additionally, there is one wide P−Fe−P angle of 136°. The origin of this large angle is not clear, but a possible explanation is increased back-bonding from a relatively electron rich Fe center into the phosphine ligands that would arise from this distortion (see SI).

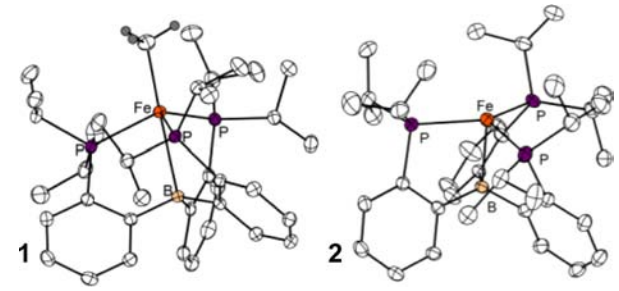

Figure 1. X-ray diffraction (XRD) structures of complexes **1** (A) and **2** (B) with hydrogen atoms and counterion (for B) omitted for clarity. See Table 1 for selected bond lengths and angles.

The Fe−B distance in **2** (2.217(2) Å) is markedly shorter than that in (TPB)FeBr (2.459(5) Å), which is noteworthy because one might expect the loss of an anionic σ-donor ligand to reduce the Lewis basicity of the metal and thus weaken the Fe−B bond. For example, the Au−B distance in (TPB)AuCl (2.318 Å) lengthens upon chloride abstraction to 2.448 Å in [(TPB)Au]$^+$.[7] To explain this difference we note that the boron center in four-coordinate **2** is less pyramidalized (Σ(C−B−C) = 347.3°) than that in five-coordinate (TPB)FeBr (Σ(C−B−C) = 341.2°), pointing to a weak interaction despite the short distance. This observation suggests that the geometry of **2** might be best understood as derived from a planar three-

Received: August 3, 2012
Published: December 21, 2012

   dx.doi.org/10.1021/ja307714m | J. Am. Chem. Soc. 2013, 135, 534−537

coordinate Fe(I) center distorted toward a T-shaped geometry,[8] the unusually short Fe−B distance being due largely to the constraints imposed by the ligand cage structure. This interpretation is consistent with a computational model study: the DFT (B3LYP/6-31G(d)) optimized geometry of the hypothetical complex $[(Me_2PhP)_3Fe]^+$ (see SI for details) exhibits a planar geometry with P−Fe−P angles of 134.8°, 113.1°, and 111.7°, very close to those measured for $[(TPB)Fe]^+$ (137.5°, 113.2°, 109.1°).

When considering the bonding of the $(Fe-B)^7$ subunit of **2** to estimate the best oxidation state and valence assignment, two limiting scenarios present themselves: Fe(III)/B(I) and Fe(I)/B(III). The structural data and computations for **2** are suggestive of a weak Fe−B interaction and indicate that this species is better regarded as Fe(I)/B(III) rather than Fe(III)/B(I). Calculations indicate that a small amount of spin density resides on the B-atom of **2** (SI) and suggest some contribution from an Fe(II)/B(II) resonance form may also be relevant. The rest of the complexes **3**−**6** presented herein possess significantly longer, and presumably weaker, Fe−B interactions (vide infra) and are hence also better classified as Fe(I) species. Additional spectroscopic studies (e.g., XAS and Mössbauer) will help to better map the Fe−B bonding interaction across the variable Fe−B distances and also the spin states of the complexes. These studies would thereby help to determine the value and limitation of classically derived oxidation/valence assignments for boratranes of these types.[9]

Table 1. Selected Metrics for Complexes 1−6

	Fe−X (Å)	Fe−B (Å)	avg Fe−P (Å)	Σ P−Fe−P	Σ C−B−C
1	2.083(10)	2.523(2)	2.40	339°	341°
2		2.217(2)	2.38	359°	347°
3	2.205(2)	2.392(2)	2.44	350°	339°
4	2.280(3)	2.433(3)	2.44	349°	341°
5	1.918(3)	2.449(4)	2.39	343°	339°
6	1.8916(7)	2.4438(9)	2.39	348°	337°

Solutions of **2** are orange in Et_2O and pale yellow-green in THF. The titration of THF into an ethereal solution of **2** results in a distinct change in the UV−vis spectrum consistent with weak THF binding. Addition of an excess of N_2H_4 to an ethereal solution of **2** results in a slight lightening of the orange color of the solution to afford $[(TPB)Fe(N_2H_4)][BAr^F{}_4]$ (**3**) in 89% yield. Complex **3** shows a paramagnetically shifted ^1H NMR spectrum indicative of an $S = 3/2$ Fe center that is corroborated by a room temperature solution magnetic moment, μ_{eff}, of 3.5 μ_B. Crystals of **3** were obtained, and XRD analysis (Figure 2A) indicates a distorted trigonal bipyramidal geometry. The Fe−N distance of 2.205(2) Å is unusually long (2.14 Å is the average quaternary N−Fe distance in the Cambridge Structural Database) reflecting its unusual quartet spin state.

Complex **3** is stable to vacuum, but solutions decompose cleanly at room temperature over hours to form the cationic ammonia complex $[(TPB)Fe(NH_3)][BAr^F{}_4]$, **4**, which was assigned by comparison of its ^1H NMR spectrum with an independently prepared sample formed by the addition of NH_3 to the cation **2**. Analysis of additional degradation products shows only NH_3 and trace H_2 (SI). The assignment of **4** as an ammonia adduct was confirmed by XRD analysis (Figure 2B). Like **3**, complex **4** shows a long Fe−N distance of 2.280(3) Å in the solid state. The complexes **2**, **3**, and **4** are unusual by virtue

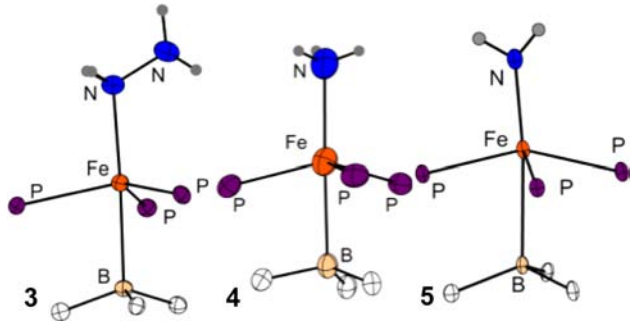

Figure 2. XRD structures of the cores of complexes **3** (A), **4** (B), and **5** (C). See Table 1 for selected distances and angles.

of their $S = 3/2$ spin states and underscore the utility of local 3-fold symmetry with respect to stabilizing high spin states at iron, even in the presence of strong-field phosphine ligands.

The addition of $NaNH_2$ to the cation **2** affords the terminal amide, (TPB)Fe−NH_2 (**5**) in ca. 85% nonisolated yield by ^1H NMR integration. The XRD structure of **5** (Figure 2C) shows an overall geometry similar to that observed in **1**, **3**, and **4**. Of interest is the short Fe−N distance of 1.918(3) Å by comparison to **4** (2.280(3) Å). The amide hydrogens were located in the difference map and indicate a nearly planar geometry about N (with the sum of the angles around N being 355°).

While the XRD data set of **5** is of high quality, we were concerned about the difficulty in distinguishing an Fe−NH_2 group from a potentially disordered Fe−OH moiety. We therefore independently characterized the hydroxo complex, (TPB)Fe−OH (**6**) (Scheme 2), which possesses a geometry

Scheme 2

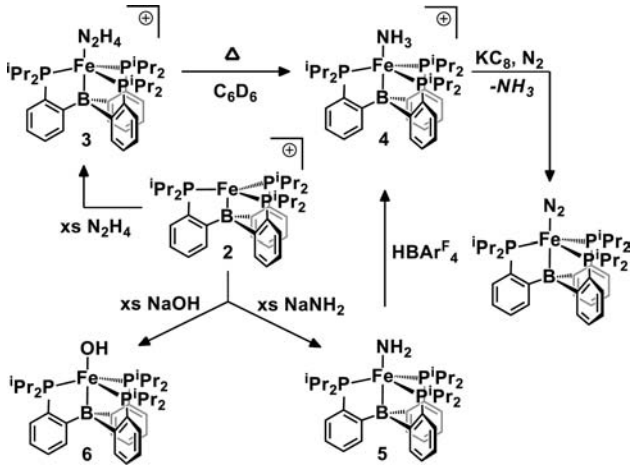

similar to that observed in **5** with an Fe−B distance of 2.4438(9) Å and an Fe−O distance of 1.8916(7) Å. Despite the structural similarity between **5** and **6**, different spectral signatures in both their ^1H NMR and EPR (Figure 3) spectra allow for facile distinction between them. Like **2**, **3**, and **4**, both **5** and **6** are $S = 3/2$.

Low-temperature EPR data (Figure 3) have been obtained on complexes **1**−**6**. All complexes show features shifted to large *g*-values consistent with quartet Fe species.[10] This assignment is verified by the solution magnetic moments obtained for these complexes. Variable temperature solid-state SQUID magnetic data for complexes **2**−**5** (SI) also establish quartet spin-state

dx.doi.org/10.1021/ja307714m | J. Am. Chem. Soc. 2013, 135, 534−537

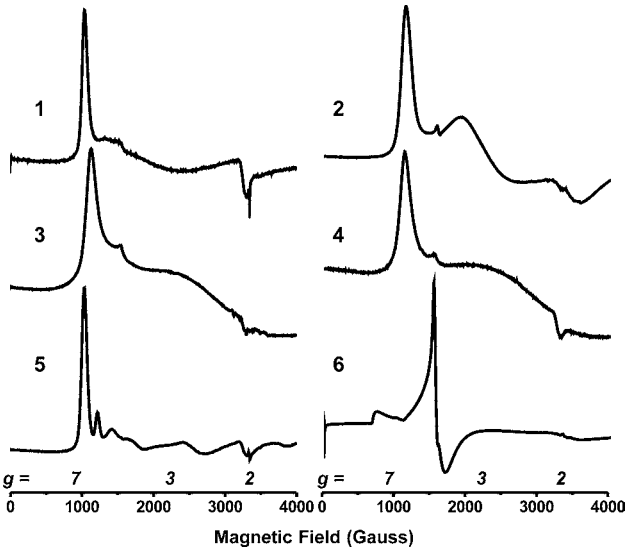

Figure 3. X-Band EPR spectra for complexes **1**–**6**. Conditions: (**1**) toluene, 8 K; (**2**) 2:1 toluene/Et_2O, 10 K; (**3**) 2-MeTHF, 10 K; (**4**) 2-MeTHF, 10 K; (**5**) 2-MeTHF, 10 K; (**6**) toluene, 10 K.

assignments and display no evidence of spin-crossover phenomena. These data show a drop in magnetic moment in the range 50–70 K for all compounds studied. We propose that this effect is due to a large zero-field splitting in these species, which is consistent with Fe centers in related geometries.[11] Simulations with zero-field splitting of 10–20 cm^{-1} provide reasonable fits to the data.

Parent amide complexes of first row transition metals are rare.[12] Noteworthy precedent for related terminal M-NH_2 species includes two square planar nickel complexes[12a,d] and one octahedral and diamagnetic iron complex, $(dmpe)_2Fe(H)$-NH_2.[12e] In addition to their different coordination numbers, geometries, and spin-states, $(dmpe)_2Fe(H)(NH_2)$ and **5** show a distinct difference at the Fe–NH_2 subunit. Six-coordinate $(dmpe)_2Fe(H)(NH_2)$ is an 18-electron species without π-donation from the amide ligand, which is pyramidalized as a result. By contrast, five-coordinate **5** accommodates π-bonding from the amide. This is borne out in its much shorter Fe–N distance (1.918(3) Å for **5** vs 2.068 Å for $(dmpe)_2Fe(H)$-(NH_2)), and also its comparative planarity (the sum of the angles around N is 355° for **5** vs 325° for $(dmpe)_2Fe(H)$-(NH_2)).

With the terminal amide **5** in hand we explored its suitability as a precursor to the previously reported N_2 complex $(TPB)Fe(N_2)$ via release of NH_3, and hence explored reduction/protonation vs protonation/reduction sequences as a means of effecting overall H-atom transfer to the Fe–NH_2 unit. Attempts to carry out the one-electron reduction of **5** were not informative. For example, electrochemical studies of **5** in THF failed to show any reversible reduction waves, but the addition of harsh reductants (e.g., *t*BuLi) to **5** did show small amounts of $(TPB)Fe(N_2)$ in the product profile. A more tractable conversion sequence utilized protonation followed by chemical reduction. Thus, the addition of $HBAr^F_4{\cdot}2Et_2O$ to **5** at low temperature (−35 °C) rapidly generates the cationic ammonia adduct **4**. The conversion is quantitative as determined by ^1H NMR spectroscopy, and **4** can be isolated in *ca.* 90% yield from the solution. Subsequent exposure of **4** to 1 equiv of KC_8 under an atmosphere of N_2 releases NH_3 and generates the $(TPB)FeN_2$ complex in similarly high yield.

In summary, an unusual series of $S = 3/2$ iron complexes featuring terminally bonded N_2H_4, NH_3, NH_2, and OH functionalities has been thoroughly characterized. These complexes are supported by a tris(phosphine)borane ligand and are best described as Fe(I) species that feature weak Fe–B bonding, though other resonance contributions to the bonding scheme warrant additional consideration. The Fe–NH_2 species faithfully models the reductive replacement of the terminal NH_2 group by N_2 with concomitant release of NH_3, lending credence to such a pathway as mechanistically feasible in Fe–mediated N_2 reduction schemes. Because spectroscopic detection of a common Fe–NH_2 or Fe–NH_3 intermediate under reductive turnover of the FeMo-cofactor has been recently proposed,[3] EPR active model complexes of the types described here should prove useful for comparative purposes.

■ ASSOCIATED CONTENT

Ⓢ Supporting Information

Detailed experimental and spectroscopic data. This material is available free of charge via the Internet at http://pubs.acs.org.

■ AUTHOR INFORMATION

Corresponding Author

jpeters@caltech.edu

Notes

The authors declare no competing financial interest.

■ ACKNOWLEDGMENTS

This work was supported by the NIH (GM 070757) and the Gordon and Betty Moore Foundation, and through the NSF via a GRFP award to J.S.A. M.-E. M. acknowledges a Fellowship for Advanced Researchers from the Swiss National Science Foundation. Larry Henling and Dr. Jens Kaiser are thanked for their assistance with X-ray crystallography and Dr. Angelo DiBilio for his assistance with EPR measurements. We acknowledge the Gordon and Betty Moore Foundation, the Beckman Institute, and the Sanofi-Aventis BRP at Caltech for their generous support of the Molecular Observatory at Caltech. SSRL is operated for the DOE and supported by its Office of Biological and Environmental Research, and by the NIH, NIGMS (including P41GM103393), and the NCRR (P41RR001209).

■ REFERENCES

(1) (a) Einsle, O.; Tezcan, F. A.; Andrade, S. L. A.; Schmid, B.; Yoshida, M.; Howard, J. B.; Rees, D. C. *Science* **2002**, *297*, 1696–1700. (b) Spatzal, T.; Aksoyoglu, M.; Zhang, L. M.; Andrade, S. L. A.; Schleicher, E.; Weber, S.; Rees, D. C.; Einsle, O. *Science* **2011**, *334*, 940–940.

(2) (a) Crossland, J. L.; Tyler, D. R. *Coord. Chem. Rev.* **2010**, *254*, 1883–1894. (b) Field, L. D.; Li, H. L.; Dalgarno, S. J.; Turner, P. *Chem. Commun.* **2008**, 1680–1682. (c) Hazari, N. *Chem. Soc. Rev.* **2010**, *39*, 4044–4056. (d) Vela, J.; Stoian, S.; Flaschenriem, C. J.; Münck, E.; Holland, P. L. *J. Am. Chem. Soc.* **2004**, *126*, 4522–4523.

(3) (a) Lukoyanov, D.; Dikanov, S. A.; Yang, Z.-Y.; Barney, B. M.; Samoilova, R. I.; Narasimhulu, K. V.; Dean, D. R.; Seefeldt, L. C.; Hoffman, B. M. *J. Am. Chem. Soc.* **2011**, *133*, 11655–11664. (b) Seefeldt, L. C.; Hoffman, B. M.; Dean, D. R. *Annu. Rev. Biochem.* **2009**, *78*, 701–722.

(4) Lee, Y.; Mankad, N. P.; Peters, J. C. *Nat. Chem.* **2010**, *2*, 558–565.

(5) (a) Betley, T. A.; Peters, J. C. *J. Am. Chem. Soc.* **2004**, *126*, 6252–6254. (b) Scepaniak, J. J.; Fulton, M. D.; Bontchev, R. P.; Duesler, E. N.; Kirk, M. L.; Smith, J. M. *J. Am. Chem. Soc.* **2008**, *130*, 10515–

10517. (c) Scepaniak, J. J.; Vogel, C. S.; Khusniyarov, M. M.; Heinemann, F. W.; Meyer, K.; Smith, J. M. *Science* **2011**, *331*, 1049−1052. (d) Scepaniak, J. J.; Young, J. A.; Bontchev, R. P.; Smith, J. M. *Angew. Chem., Int. Ed.* **2009**, *48*, 3158−3160.
(6) Moret, M.-E.; Peters, J. C. *Angew. Chem., Int. Ed.* **2011**, *50*, 2063−2067.
(7) Sircoglou, M.; Bontemps, S.; Bouhadir, G.; Saffon, N.; Miqueu, K.; Gu, W.; Mercy, M.; Chen, C.-H.; Foxman, B. M.; Maron, L.; Ozerov, O. V.; Bourissou, D. *J. Am. Chem. Soc.* **2008**, *130*, 16729−16738.
(8) A stable T-shaped, three-coordinate Fe(I) is known: Ingleson, M. J.; Fullmer, B. C.; Buschhorn, D. T.; Fan, H.; Pink, M.; Huffman, J. C.; Caulton, K. G. *Inorg. Chem.* **2008**, *47*, 407−409.
(9) (a) Amgoune, A.; Bourissou, D. *Chem. Commun.* **2011**, *47*, 859−871. (b) Hill, A. F.; Owen, G. R.; White, A. J. P.; Williams, D. J. *Angew. Chem., Int. Ed.* **1999**, *38*, 2759−2761. (c) Pang, K.; Quan, S. M.; Parkin, G. *Chem. Commun.* **2006**, 5015−5017.
(10) Stoian, S. A.; Yu, Y.; Smith, J. M.; Holland, P. L.; Bominaar, E. L.; Munck, E. *Inorg. Chem.* **2005**, *44*, 4915−4922.
(11) Harman, W. H.; Harris, T. D.; Freedman, D. E.; Fong, H.; Chang, A.; Rinehart, J. D.; Ozarowski, A.; Sougrati, M. T.; Grandjean, F.; Long, G. J.; Long, J. R.; Chang, C. J. *J. Am. Chem. Soc.* **2010**, *132*, 18115−18126.
(12) (a) Adhikari, D.; Mossin, S.; Basuli, F.; Dible, B. R.; Chipara, M.; Fan, H.; Huffman, J. C.; Meyer, K.; Mindiola, D. J. *Inorg. Chem.* **2008**, *47*, 10479−10490. (b) Brady, E.; Telford, J. R.; Mitchell, G.; Lukens, W. *Acta Cryst. C* **1995**, *51*, 558−560. (c) Redshaw, C.; Wilkinson, G.; Hussain-Bates, B.; Hursthouse, M. B. *J. Chem. Soc. Dalton* **1992**, 1803−1811. (d) Cámpora, J.; Palma, P.; del Río, D.; Conejo, M. M.; Álvarez, E. *Organometallics* **2004**, *23*, 5653−5655. (e) Fox, D. J.; Bergman, R. G. *J. Am. Chem. Soc.* **2003**, *125*, 8984−8985. (f) Sofield, C. D.; Walter, M. D.; Andersen, R. A. *Acta Cryst. C* **2004**, *60*, 465−466.